Journal of the Ceramic Society of Japan 117 [11] 1258-1262 2009 **Paper**

Sintering, microstructural and mechanical characterization of combustion synthesized Y_2O_3 and Yb^{3+}–Y_2O_3

Ramalinga Viswanathan MANGALARAJA,† Solaiappan ANANTHAKUMAR,* Johanne MOUZON, Marta LÓPEZ, Carlos Porro CAMURRI and Magnus ODÉN****

Department of Materials Engineering, University of Concepción, Casilla 160-C, Concepción, Chile
***Materials and Minerals Division, National Institute for Interdisciplinary Science and Technology (NIIST), CSIR, Trivandrum, Kerala - 695 019, India**
****Division of Engineering Materials, Luleå University of Technology, SE-971 87, Luleå, Sweden**

The present work highlights the microstructural features and mechanical properties of Y_2O_3 prepared with and without Yb^{3+} doping that processed through combustion synthesis involving various organic fuels such as urea, citric acid and glycine. Properties such as powder-flow, particle packing, green density, % of shrinkage, sintered density, grain size, Vicker's microhardness (H_v) and fracture toughness (K_{IC}) were analyzed and compared with respect to the fuel sources. The as combusted precursors were calcined at 1100°C for 4 h under oxygen atmosphere to obtain fully crystalline Y_2O_3 powders. Cylindrical pellets were fabricated as test specimens and sintered at 1600°C for 3 h. The SEM images of the sintered yttria samples show an average grain size of < 3 μm irrespective of the fuels. However, the mechanical properties show significant dependence on the fuels used. A maximum hardness of 6.8 ± 0.1 and 7.0 ± 0.1 GPa was obtained for Y_2O_3 and Yb^{3+} doped Y_2O_3 derived from glycine fuel. Whereas the maximum fracture toughness of 2.6 ± 0.3 MPa $m^{1/2}$ was obtained for the samples derived from urea. The Yb^{3+} doping found to increase the bulk hardness of yttria from 0.2 to 0.6 GPa. The study contributes to appropriately select the fuels for obtaining high dense, mechanically stable yttria ceramics through combustion process.

Key-words : Combustion, Organic fuels, Yttria, Ytterbium, Mechanical properties, Sintering

[Received April 21, 2009; Accepted September 11, 2009]

1. Introduction

Yttria ceramics have been gaining significant importance in applied electronics and optical fields. Yttria has excellent physical and chemical properties such as high melting point, ≅ 2410°C, low vapour pressure, optical transparency over a wide region and high corrosion resistance.[1)] These properties suggest that it is a promising material for a range of applications as high temperature chemically-resistant substrates, crucibles for melting reactive metals, nozzles for jet-casting melt and rare-earth-iron magnetic alloys.[2)–4)] Polycrystalline ytterbium (Yb^{3+}) doped yttria is recommended recently as a novel material for solid state lasers. Yb^{3+} is an active ion exhibits both high power and efficiency due to its small quantum defect and hence used in laser-diode pumping.[5),6)] Processing of Y_2O_3 ceramics with different dopant ions is actively taken up in our research through combustion processing mainly to synthesize low temperature sinterable, yttria powders. Infact, the common factors that influence densification as well as the final sintered microstructures include: (i) starting precursor/powder materials characteristics: (a) particle size and its distribution (b) degree of agglomeration (c) particle shape (d) crystalline defects (e) adsorbed ions (f) impurities (g) homogeneity in the case of multicomponent system, (ii) packing of the powder (compaction) in the green body and (iii) thermal treatment (drying, calcination and sintering).[2),7)] We have been conducting series of experiments on combustion synthesis of polycrystalline yttria powders with and without selective dopants using organic fuels in order to study the effect of fuels on the resultant powder characteristics including morphology, surface area, particle size and distribution. We have already reported the combustion synthesis of Y_2O_3 and Yb^{3+} doped Y_2O_3 and their powder characteristics.[8)] In this work, we have presented the physical properties such as powder packing, sintering, microstructural features and associated mechanical properties. In addition to that, the results on tap density, bulk density and sintering shrinkage and porosity were also studied and reported.

2. Experimental procedure

Phase pure and thermally reactive yttria powders were prepared by combustion method using yttrium nitrate with various organic fuels such as urea, citric acid and glycine. Yttria having 25 mol% Yb^{3+} ions was prepared in order to analyze the dopant distribution and its influence on microstructural and mechanical properties of the sintered ceramics.[9)] The details on combustion synthesis are already described in our earlier report.[8)] All the yttria powders derived in the as-prepared conditions were calcined at 1100°C for 4 h[1),2),10)] in oxygen atmosphere at the flowing rate of 70–100 mL/min to obtain single phase cubic yttria. The obtained yttria powders as well as the sintered yttria ceramics were designated according to the types of fuels. The undoped yttria samples were designated as U-YO (urea), C-YO (citric acid) and G-YO (glycine). Similarly, the Yb^{3+} doped yttria samples were designated as U-YbYO, C-YbYO and G-YbYO.

The tap density (g/ml) was measured to analyze the powder-flow and compressibility properties. The maximum packing den-

† Corresponding author: R. V. Mangalaraja; E-mail: mangal@udec.cl

sity of the powder was determined under the influence of well-defined externally applied force. A known amount of Y_2O_3 powder was taken in a plastic measuring cylinder and then dropped for hundred times from a constant height to achieve minimum packed volume.

Y_2O_3 test specimens were fabricated as cylindrical discs with thickness t = 3 mm and diameter D = 14 mm using an uni-axial press at a pressure of 30 MPa. The pressed discs were again subjected to cold iso-static pressing (CIP) at a pressure of 200 MPa. Green densities for both uni-axially and cold iso-statically pressed samples were determined from the geometrical measurements. The samples were sintered at a temperature of 1600°C for 3 h in the air atmosphere. The sintered properties such as bulk density, true density, % sintering shrinkage and porosity were measured by Archimedes principle. In each set, 12 samples were used for determining the density values.

The sintered samples were carefully diamond polished to produce optical finish. The Vicker's hardness was measured at room temperature using Struers hardness tester. The hardness was calculated from the ratio between the applied load via a geometrically defined indenter and the contact (projected) area of the resultant impression using the relation:

$$H_v = 1854.4\ P/d^2\ (GPa)$$

where H_v is the Vicker's hardness (GPa), P is the applied load (kg) and 'd' is the indentation diagonal length (mm). In the indentation hardness tests, load was varied from 1 N to 20 N. The indentation time was fixed as 10 seconds. Six to eight indentations were made in all the samples at the given loads. The fracture toughness which characterizes the resistance of a material to crack propagation or to damage (including mechanical and thermal shock) was determined by the indentation technique using the hardness tester. The fracture toughness of the sintered yttria and ytterbium doped yttria ceramics was determined at a fixed load of 10 N. Both crack lengths and diagonal lengths of the indentation were measured first and then the fracture toughness (K_{IC}) values were calculated using the formula:[11)]

$$K_{IC} = 0.16\ H_v\ a^2c^{-3/2}\ (MPa\ m^{1/2})$$

where H_v is the Vicker's hardness, 'a' and 'c' are diagonal and crack length generated by the indentation. The typical indentation marks generated on the polished surface were also captured using scanning Electron Microscope (SEM). The microstructural features of the sintered Y_2O_3 were also viewed on the fractured mode using SEM (SEM, JEOL Ltd., JSM 6460 LV).

3. Results and discussion

3.1 Physical characterization

The physical characteristics of the combustion synthesized yttria and Yb^{3+} doped Y_2O_3 powders are presented in **Table 1**. The tap density values are indicative of the powder-flow behavior and it can be seen that the Y_2O_3 powders derived from the urea and citric acid fuels have the values close to each other compared to glycine derived counterpart. A marginal increase in the tap density is noticed for glycine under identical conditions. In the case of Yb^{3+} doped yttria, the tap density, green density, % of shrinkage (before and after cold iso-static pressing) values follow a general trend as low tap density, high green density and less % shrinkage.

When the powder flow largely depends on its morphology, the particle packing is influenced mainly by morphology as well as particle size and distribution. In our earlier work we reported the morphology variations of the combustion synthesized Yb^{3+} doped Y_2O_3 powders with respect to various fuels. We obtained morphologies as spongy particles, platelets and flaky types in the as-prepared powders.[8)] The spongy nature was observed in glycine fuels whereas the citric acid and urea fuels had soft agglomerated clusters with spherical and platy particles.

Spongy powders contain physically hindered nano crystals due to strong inter-particle forces. In such nano crystals pore to particle size ratio is less and therefore during taping they have attained increased packing leading to high tap density value. However, this is not reflected in the green density values as expected. It is known that the nano particles are difficult to compress under simple uniaxial pressing. They usually exhibit better packing under compression but once the applied pressure is released, significant relaxation occurred due to the inherent visco-elastic character that ultimately lower the green density. This behaviour is invariably noticed in sol gel derived nano particulate silica and alumina [boehmite phase] particles. In our case we have seen nano range Y_2O_3 particles in glycine derived powders. They showed poor packing under simple uniaxial pressing which was also confirmed by its excessively high % shrinkage during CIP process. In this case also the visco-elastic relaxation is one of the reasons for low green density. In the case of citric acid and urea fuels, the soft agglomerates contain wide particle size distributions of spherical and platy particles. Such agglomerates show improper flow and irregular arrangements during packing finally result in low tap density. However at elevated pressures, the soft agglomerates are disintegrated and get com-

Table 1. Physical Characterization of Yttria and Ytterbium Doped Yttria Before Sintering

S. No	Sample Name	Tap Density (%)	Green density after uni-axial pressing (by geometrical measurement) (%)	Green density after CIP (by geometrical measurement) (%)	Shrinkage after CIP (%)
1	YO-Urea	1.21 (23.96)	1.92 (38.26)	2.57 (51.08)	25.93
2	YbYO-Urea	0.881 (13.95)	2.18 (37.65)	2.84 (48.98)	23.51
3	YO-Citric Acid	1.231 (24.47)	1.90 (37.77)	2.61 (51.94)	27.28
4	YbYO-Citric Acid	1.126 (17.84)	2.14 (36.92)	2.90 (49.99)	26.09
5	YO-Glycine	1.295 (25.75)	1.73 (34.48)	2.47 (49.04)	29.70
6	YbYO-Glycine	1.123 (17.79)	2.02 (34.92)	2.77 (47.78)	26.81

The percentage of theoretical density is given in the parenthesis.

pressed firmly resulting in good packing. Since they do not obey the visco-elastic relaxation, high green density and low % shrinkage are finally attained. When Yb^{3+} doping is employed, the powders contain high volume fractions of fine-particles irrespective of the fuels and therefore obviously show close packing leading to high green density and less green shrinkage. The packing properties of the Y_2O_3 and Yb^{3+} doped Y_2O_3 powders seen for the different organic fuels show direct influence on the sintered properties of the Y_2O_3 ceramics.

The physical characteristics of the sintered Y_2O_3 and Yb^{3+} doped Y_2O_3 powders are presented in **Table 2**. Infact from Table 1 we found that among urea, citric acid and glycine fuels, the theoretical green density was comparatively high in urea and citric acid derived powders. Therefore we expected that these powders may show better densification upon sintering. However, on the contrary, the yttria green compacts derived from these fuels showed theoretical sintered density only up to 90% at 1600°C. The sintered densities were high for glycine derived Y_2O_3 ceramics. In this case, maximum theorectical sintered densities of 98.2% and 96.5% were obtained for Y_2O_3 and Yb^{3+} doped Y_2O_3 ceramics, respectively. It again confirms the nanonature of the glycine derived Y_2O_3 powders.

The glycine derived sintered yttria also exhibits significantly low bulk porosities and it is only less than 5%. These results indicate that the glycine fuel is better for obtaining sinter-active Y_2O_3 powders. The sintered densities and porosities obtained in this work are better than the values reported earlier.[12)–14)] The study shows that although the powder morphology play a critical role in deciding the flow and packing properties of Y_2O_3 powders, the Y_2O_3-densification mainly depends on the ultimate particle size. Hence fine-Y_2O_3 particles should invariably be achieved for low temperature densification and sintered grain size < 1 μm. In most of the earlier works a sintering temperature of above 1600°C was employed for achieving 99% dense sintered yttria ceramics. In this study we have shown that morphology also should be critically controlled in addition to the particle size and distribution so that a proper flow and high packing during compaction and subsequently 99% dense Y_2O_3 could be achieved upon sintering.

Another factor affecting the densification is the initial calcination temperatures and heating schedule. The particle growth and agglomeration are primarily evolved during calcination. It is already reported that in chemically synthesized Y_2O_3 precursors the skeleton of the particles dissociated into monodispersed particles which produced highly sinterable yttria when the calcination temperature is greater than 1000°C.[1),8)] The calcination treatment causes an internal structural reorganization within the primary particles (grain crystallization) and thus reducing the surface free-energy that result in low- temperature densification.[1),15)] In our study, we calcined the powders at 1100°C and found that the green compacts attained significantly high densification at a given sintering temperature of 1600°C. The sintered Y_2O_3 samples showed open porosity < 5% for the fuels. However the % closed porosity was found to be excessively high in the citric acid and urea fuels. The differential rate of lattice diffusion of Y^{3+} and Yb^{3+} ions and grain growth kinetics[16)] vary with respect to the combustion efficiency of the fuel causing variations in the % closed pores with respect to the fuels. Infact, the removal of the entrapped pores usually required high sintering temperatures. The closed pores could be removed only when the grains were allowed to grow excessively larger either by increasing the sintering temperatures or extending the soaking duration. In our cases we have purposefully avoided sintering temperature above 1600°C and that unfortunately resulted in high % closed porosity. However at this temperature the glycine derived yttria samples showed closed pores only less than 2%. It indicates that one can achieve sintering close to the theoretical density if the fuel selection is made properly for the combustion synthesis of Y_2O_3.

In presence of Yb^{3+}, the densification is slow and hence the % open porosity is more in all the cases. Ytterbium oxide being a rare earth family has unusually high melting temperature and recommended mostly as an additive to control the grain growth. Being a high temperature rare earth oxide, the given sintering temperature is infact inadequate to induce accelerated rate of densification. Also, Yb^{3+} ions show diffusivities along the lattice and grain boundaries whereas Y^{3+} ions have self diffusivity during densification.

3.2 Microstructure

The microstructural images of the as-sintered (1600°C/3 h) Y_2O_3 and Yb^{3+} doped yttria samples are shown in **Fig. 1**. The microstructures were taken on fractured mode and the SEM images revealed inter-granular fracture that indicates the sintered ceramic has weak grain boundaries. There is not much difference in the average sintered grain sizes between Y_2O_3 and Yb^{3+} for all the fuel sources and it is observed that the average grain sizes fall below 3 μm. We expected comparatively smaller grain size in the Yb^{3+} ions doped yttria samples. Since the doping caused negative effect in the powder flow and particle packing overall, similar influence is also noticed in the grain size. The microstructures correspond to Y_2O_3 derived from urea and citric acid fuels contain pores at the grain boundaries. Glycine derived Y_2O_3 samples

Table 2. Physical Characterization of Yttria and Ytterbium Doped Yttria After Sintering

S. No	Sample Name	Sintered density (by geometrical measurement) (%)	Shrinkage after sintering (%)	Sintered density (by Archimedes principle) (%)	Open porosity (%)	Closed porosity (%)
1	YO-Urea	4.41 (87.72)	57.29	4.59 (91.17)	3.45	8.83
2	YbYO-Urea	5.10 (87.95)	57.89	5.06 (87.27)	–	12.73
3	YO-Citric Acid	4.50 (89.54)	58.40	4.71 (93.58)	4.04	6.42
4	YbYO-Citric Acid	5.16 (89.10)	59.11	5.29 (91.26)	2.16	8.74
5	YO-Glycine	4.81 (95.62)	64.42	4.94 (98.18)	2.56	1.82
6	YbYO-Glycine	5.48 (94.58)	63.54	5.59 (96.48)	1.90	3.52

The percentage of theoretical density is given in the parenthesis.

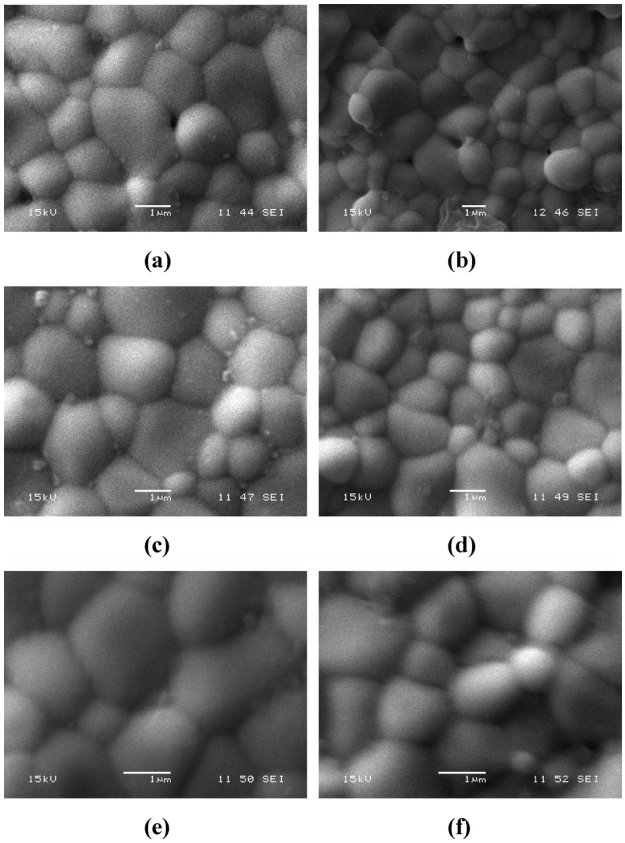

Fig. 1. SEM photographs of the as-sintered (at 1600°C for 3 h) surfaces of yttria and ytterbium doped yttria prepared using urea, citric acid and glycine. (a) U-YO, (b) U-YbYO, (c) C-YO, (d) C-YbYO, (e) G-YO and (f) G-YbYO.

showed comparatively dense microstructures and relatively smaller grain size. SEM observations clearly show that an appropriate fuel source is important in the beginning itself for the combustion process, such as glycine for having controlled microstructures.

3.3 Mechanical properties

The hardness Vs load curves for the doped and undoped sintered yttria ceramics is shown in **Fig. 2** for all the fuels. The hardness appears to be grain size independent and it gradually increased with the applied load from 1 N to 20 N. Hardness varies usually with grain size and it is earlier reported that a dense fine grained yttria produced by aerosol technique has H_v values 7.7 GPa for the film and 6.7 GPa for the bulk.[17),18)] Smaller grains resist plastic deformation and result in high hardness even at higher loads. In our work, the sintered yttria ceramics fabricated from urea-combustion showed the average hardness value asH_v = 4.6 GPa at 10 N. At this load the classical indentation image was unambiguous. The H_v values 5.2 and 6.3 GPa are obtained for citric acid and glycine fuels respectively at 10 N. The dispersions in the hardness values for urea, citric acid and glycine derived yttria at 10 N are 4.46 to 4.73 GPa, 5.19 to 5.36 GPa and 6.23 to 6.34 GPa, respectively. Because we obtained comparatively similar microstructural homogeneity, and average grain size, the microstructural features other than grain size has to be taken into consideration for interpreting the hardness values. We have already seen high green density, poor densification and high % closed porosity as characteristics of yttria powders derived from urea and citric acid fuels. In sintered ceramics, the indentation damage is generated by plastic deformation and when the material contains closed porosity, the deformation damage is directly proportional to the applied stress. Therefore defects such as closed pores and poor densification are the main reasons for the low hardness in urea and citric acid fuels. As expected the hardness is high for the glycine derived yttria samples due to its high sintered density. The Yb^{3+} doping contributes to enhance the hardness marginally. The observed hardness values are in good agreement with the hardness values reported earlier for hot isostatically pressed and vacuum sintered yttria samples.[19),20)]

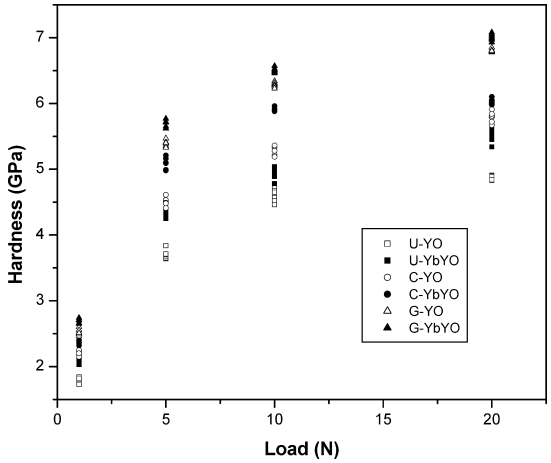

Fig. 2. Dependence of hardness on applied load for sintered yttria and ytterbium doped yttria ceramics prepared using urea, citric acid and glycine.

Table 3. Mechanical Hardness and Fracture Toughness of the Yttria and Ytterbium Doped Yttria Under the Applied Load 10 N

S. No	Sample name	Hardness (GPa)	Fracture toughness (MPa $m^{1/2}$)
1	YO-Urea	4.6 ± 0.15	1.4 ± 0.2
2	YbYO-Urea	4.9 ± 0.15	2.6 ± 0.3
3	YO-Citric Acid	5.2 ± 0.15	1.4 ± 0.1
4	YbYO-Citric Acid	5.8 ± 0.15	2.2 ± 0.2
5	YO-Glycine	6.3 ± 0.1	1.1 ± 0.1
6	YbYO-Glycine	6.5 ± 0.1	1.3 ± 0.1

Measured at the applied load of 10 N.

The fracture toughness values determined by indentation method at a constant load of 10 N are given along with the hardness in **Table 3**. Earlier studies reported a fracture toughness of dense yttria as 2.8 MPa $m^{1/2}$. In our case compared to undoped Y_2O_3, the doped samples showed increased trend in the fracture toughness for all the fuels. A maximum fracture toughness is value of 2.6 ± 0.3 MPam$^{1/2}$ is obtained in Yb^{3+} doped yttria samples derived from urea. Fracture toughness is said to be a grain boundary phenomenon. Due to theoretical density differences between yttria and ytterbia, Yb^{3+} ions possibly get segregated along the grain boundaries and strengthen the same. It leads to marginal increase in the toughness values. Since the glycine derived yttria has high density, it shows high hardness but low fracture toughness compared to other fuels. The indentation

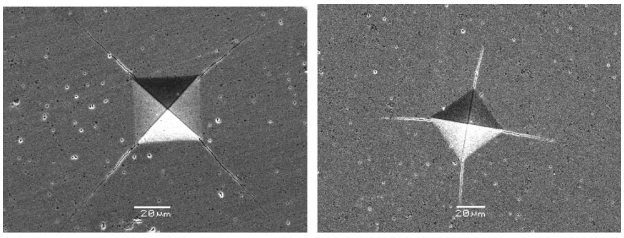

(a) G-YO (b) G-YbYO

Fig. 3. Indentation photographs of pure and ytterbium doped yttria prepared using Glycine (a) G-YO and (b) G-YbYO.

mark images and the developed cracks are shown in **Fig. 3** for the Y_2O_3 and Yb^{3+} doped yttria samples derived from glycine fuel. The fracture toughness values of yttria ceramics obtained in the present work are in accordance with the reported results.[19),21)]

4. Conclusions

In the present work the powder characteristics of Y_2O_3 and Yb^{3+} doped yttria ceramics derived through combustion technique using different organic fuels namely urea, citric acid and glycine have been studied and correlated with the sintering and mechanical properties. Fully crystalline, single phase Y_2O_3 and Yb^{3+} doped yttria has been obtained at 1100°C. Out of the three organic fuels, yttria powders derived through urea and citric acid fuels exhibit less powder-flow but increased theoretical green density. However, they attained only low theoretical sintered density under identical conditions. The yttria powders prepared using glycine fuels contained nano scale particles eventually showed increased particle packing and therefore increased densification. A theoretical density of 98.2% and 96.5% has been respectively obtained at 1600°C for the sintered Y_2O_3 and Yb^{3+} doped yttria prepared using glycine. Yb^{3+} doping has no significant effect on densification but marginal advantage in the mechanical properties. In all the cases, the average sintered grain size of below 3 μm was obtained. The highest hardness of 6.8 ± 0.1 and 7.0 ± 0.1 GPa is obtained for the glycine prepared Y_2O_3 and Yb^{3+} doped yttria, respectively. A maximum fracture toughness of 2.6 ± 0.3 $MPam^{1/2}$ is obtained for Yb^{3+} doped yttria prepared using urea.

Acknowledgement One of the authors R. V. Mangalaraja would like to thank Direction of Investigation, University of Concepción and FONDECYT (No: 11060302), Govt. of Chile, Santiago for financial assistance.

References

1) T. Ikegami, J.-G. Li and T. Mori, *J. Am. Ceram. Soc.*, 85, 1725–1729 (2002).
2) A. L. Micheli, D. F. Dungan and J. V. Mantese, *J. Am. Ceram. Soc.*, 75, 709–711 (1992).
3) F. Jollet, C. Noguera, N. Thromat, M. Gautier and J. P. Duraud, *Phys. Review B*, 42, 7587–7595 (1990).
4) S. V. Chavan, K. T. Pillai and A. K. Tyagi, *Scrip. Mater.*, 132, 569–572 (2006).
5) K. Takaichi, H. Yagi, J. Lu, J.-F. Bisson, A. Shirakawa, K. Ueda, T. Yanagitani and A. A. Kaminskii, *Appl. Phys. Lett.*, 84, 317–319 (2004).
6) A. Shirakawa, K. Takaichi, H. Yagi, J.-F. Bisson, J. Lu, M. Musha, K. Ueda, T. Yanagitani, T. S. Petrov and A. A. Kaminskii, *Opt. Exp.*, 11, 2911–2916 (2003).
7) A. L. Micheli, *Ceram. Int.*, 15, 131–139 (1989).
8) R. V. Mangalaraja, J. Mouzon, P. Hedström, I. Kero, K. V. S. Ramam, C. P. Camurri and M. Odén, *J. Mater. Proc. Tech.*, 208, 415–422 (2008).
9) G. Boulon, L. Laversenne, C. Goutaudier, Y. Guyot and M. T. Cohen-Adad, *J. Lumin.*, 102–103, 417–425 (2003).
10) L. Wen, X. Sun, Z. Xiu, S. Chen and C.-T. Tsai, *J. Eur. Ceram. Soc.*, 24, 2681–2688 (2004).
11) A. G. Evans and E. A. Charles, *J. Am. Ceram. Soc.*, 59, 371–372 (1976).
12) A. Dupont, A. Largeteau, C. Parent, B. Le Garrec and J. M. Heintz, *J. Eur. Ceram. Soc.*, 25, 2007–2013 (2005).
13) N. Dasgupta, R. Krishnamoorthy and K. T. Jacob, *Int. J. Inorg. Mater.*, 3, 143–149 (2001).
14) S. V. Chavan, K. T. Pillai and A. K. Tyagi, *Mater. Sci. Engi. B*, 132, 266–271 (2006).
15) A. Dupont, C. Parent, B. L. Garrec and J. M. Heintz, *J. Solid State Chem.*, 171, 152–160 (2003).
16) Z. Huang, X. Sun, Z. Xiu, S. Chen and C.-T. Tsai, C.-T. Tsai, *Mater. Lett.*, 58, 2137–2142 (2004).
17) J. Iwasawa, R. Nishimizu, M. Tokita and M. Kiyohara, *J. Am. Ceram. Soc.*, 90, 2327–2332 (2007).
18) A. Senthil Kumar, A. Raja Durai and T. Sornakumar, *Mater. Lett.*, 58, 1808–1810 (2004).
19) M. Desmaison-Brut, J. Montintin, F. Valin and M. Boncoeur, *J. Am. Ceram. Soc.*, 78, 716–722 (1995).
20) T. Tani, Y. Miyamoto, M. Koizumi and M. Shimada, *Ceram. Int.*, 12, 33–37 (1986).
21) G. Fantozzi, G. Orange, K. Liang, M. Gautier, J.-P. Duraud, P. Maire, C. L. Gressus and E. Gillet, *J. Am. Ceram. Soc.*, 72, 1562–1563 (1989).